

AN ADAPTIVE SURFACE FINITE ELEMENT METHOD BASED ON VOLUME MESHES*

ALAN DEMLOW[†] AND MAXIM A. OLSHANSKII[‡]

Abstract. In this paper we define an adaptive version of a recently introduced finite element method for numerical treatment of elliptic PDEs defined on surfaces. The method makes use of a (standard) outer volume mesh to discretize an equation on a two-dimensional surface embedded in \mathbb{R}^3 . Extension of the equation from the surface is avoided, but the number of degrees of freedom (d.o.f.) is optimal in the sense that it is comparable to methods in which the surface is meshed directly. In previous work it was proved that the method exhibits optimal order of convergence for an elliptic surface PDE if the volume mesh is uniformly refined. In this paper we extend the method and develop an a posteriori error analysis which admits adaptively refined meshes. The reliability of a residual type a posteriori error estimator is proved and both reliability and efficiency of the estimator are studied numerically in a series of experiments. A simple adaptive refinement strategy based on the error estimator is numerically demonstrated to provide optimal convergence rate in the H^1 norm for solutions with point singularities.

Key words. surface, interface, finite element, level set method, adaptivity, error estimator

AMS subject classifications. 65N15, 65N30

DOI. 10.1137/110842235

1. Introduction.

1.1. Background. Partial differential equations (PDEs) posed on surfaces arise in mathematical models for many natural phenomena: diffusion along grain boundaries, lipid interactions in biomembranes, and transport of surfactants on multiphase flow interfaces, to mention a few. Recently there has been significant interest in developing and analyzing numerical methods for the solution of PDEs on surfaces. We briefly mention some important developments related to the approach studied in this paper.

The paper of Dziuk [12] contains the first analysis of a finite element method (FEM) for the Laplace–Beltrami equation on a stationary surface. In that method the surface Γ is approximated by a regular family $\{\Gamma_h\}$ of consistent triangulations. It is assumed that all vertices in the triangulations lie on Γ . The finite element space then consists of scalar functions that are continuous on Γ_h and linear on each triangle in the triangulation Γ_h . If the surface evolves, then its triangulations and finite element spaces have to be rebuilt. The method has recently been extended from linear to higher order finite elements in [9]. An adaptive finite element version of the method (AFEM) based on linear finite elements and suitable a posteriori error estimators is treated in [8]. In [13] the approach from [12] has been extended to parabolic equations on a stationary surface, and in [15] the method is combined with Lagrangian surface tracking and is generalized to equations on evolving surfaces.

*Received by the editors July 25, 2011; accepted for publication (in revised form) February 24, 2012; published electronically June 19, 2012.

<http://www.siam.org/journals/sinum/50-3/84223.html>

[†]Department of Mathematics, University of Kentucky, Lexington, KY 40506-0027 (alan.demlow@uky.edu). This author's work was partially supported by National Science Foundation grant DMS-1016094.

[‡]Department of Mechanics and Mathematics, M.V. Lomonosov Moscow State University, Moscow 119899, Russia (Maxim.Olshanskii@mtu-net.ru). This author's work was partially supported by the German Research Foundation and the Russian Foundation for Basic Research through projects 12-01-91330 and 11-01-00971.

In order to avoid remeshing and make full use of the implicit definition of the surface as the zero of a level set function, it was first proposed in [5] to extend the PDE from the surface to a set of positive Lebesgue measure in \mathbb{R}^3 . The resulting PDE is then solved in one dimension higher but can be solved on a mesh that is unaligned to the surface, leading to an Eulerian technique. In that paper, finite difference approximations on rectangular grids independent of a static surface are considered. The approach was further developed in [1, 17] for finite difference approximations including moving surfaces. An FEM based on extension of the surface equation was proposed and developed in [6]. A related finite element approach was studied in [7] and [14].

Another new Eulerian technique for the numerical solution of an elliptic equation posed on a hypersurface in \mathbb{R}^3 was introduced in the recent paper [22]. The main idea of the method, defined formally in the next section, is to use finite element spaces that are induced by the volume triangulations (tetrahedral decompositions) of a bulk domain in order to discretize the PDE on the embedded surface. However, in contrast to the Eulerian method from [5] this method does not use an extension of the surface PDE. It is instead based on a restriction (trace) of the outer finite element spaces to the discrete surface. This leads to discrete problems for which the number of degrees of freedom (d.o.f.) conforms with the two-dimensional nature of the surface problem, similar to the Lagrangian approach from [12]. At the same time, the method is essentially Eulerian as a surface is not tracked by a mesh and may be defined implicitly as the zero of a level set function. If the surface evolves, one must recompute the surface mass and stiffness matrices, using the same data structures each time. This feature is attractive from the implementation point of view. Algebraic properties of the method were studied in [23].

In [22] it was proved that this surface FEM has optimal order of convergence in the H^1 and L^2 norms for elliptic surface PDEs if the volume mesh is uniformly refined. In the present paper, we study the method for the case of locally refined meshes. Our main theoretical result is a residual-type a posteriori upper bound for the finite element error in the H^1 norm. We note that the analytical technique in this paper is largely different from that of [22]. As explained in section 2.6, the latter appears problematic to extend to the case of locally refined meshes. Our analysis is also more delicate than standard proofs for the Euclidean case or the previously studied case of surface FEM with regular surface triangulations (cf. [8]). The main analytical challenge here is the fact that the surface mesh inherited from the bulk mesh is highly irregular, so tools from approximation theory, inverse estimates, etc., may for the most part only be applied on the bulk mesh.

1.2. Summary of results. For clarity, in this work we consider the Laplace–Beltrami equation

$$(1.1) \quad -\Delta_{\Gamma} u = f \text{ on } \Gamma.$$

Here Γ is a closed C^2 surface embedded in \mathbb{R}^3 , and $\int_{\Gamma} f \, ds = 0 = \int_{\Gamma} u \, ds$ are enforced in order to guarantee existence and uniqueness of solutions to u , respectively. Also, $\Delta_{\Gamma} = \nabla_{\Gamma} \cdot \nabla_{\Gamma}$, where ∇_{Γ} is the tangential gradient on Γ . Our results can be extended to more general elliptic surface equations in a standard way. In this case, generic constants from the corresponding estimates would depend on constants from the ellipticity and continuity conditions for the bilinear form of the elliptic problem at hand.

Next we briefly describe our error estimators. An element T of the surface mesh is the (arbitrary) intersection of a plane with a tetrahedron S . (Precise definitions

are given below.) It is natural to question whether the area $|T|$ of the surface element or the corresponding quantity h_T^2 (with $h_T = \text{diam}(S)$) derived from the parent tetrahedron should be used in order to measure mesh size, since in contrast to the case of regular meshes it sometimes occurs that $|T| \ll h_T^2$. We accordingly define a family of residual-type error indicators,

$$(1.2) \quad \eta_p(T) = C_p \left(|T|^{1/2-1/p} h_T^{2/p} \|f_h + \Delta_{\Gamma_h} u_h\|_{L_2(T)} + \sum_{e \subset \partial T} |e|^{1/2-1/p} h_T^{1/p} \|[\![\nabla_{\Gamma_h} u_h]\!] \|_{L_2(e)} \right), \quad p \in [2, \infty].$$

Here u_h is the finite element solution defined with respect to an approximation f_h to f , and e denotes an edge of the element T . When $p = 2$, this reduces to the expression $\eta_2(T) = C_2(h_T \|f_h + \Delta_{\Gamma_h} u_h\|_{L_2(T)} + h_T^{1/2} \|[\![\nabla_{\Gamma_h} u_h]\!] \|_{L_2(\partial T)})$ in which the diameter of the outer tetrahedron is used to measure the mesh size. At the other extreme $p = \infty$, we have instead the expression $\eta_\infty(T) = C_\infty(|T|^{1/2} \|f_h + \Delta_{\Gamma_h} u_h\|_{L_2(T)} + \sum_{e \subset \partial T} |e|^{1/2} \|[\![\nabla_{\Gamma_h} u_h]\!] \|_{L_2(e)})$ in which the properties of the surface element T are used in a sharp fashion to measure local mesh size. For $p \in [2, \infty)$, we show reliability up to geometric terms of the a posteriori estimators obtained by suitably summing these local contributions over the mesh. In our theory the constant C_p blows up as $p \rightarrow \infty$ and the limit case $p = \infty$ is thus excluded. A major conclusion of this work is that while taking $p > 2$ seems to allow for sharper accounting of the variations of the surface mesh properties, the performance of the coarsest indicators η_2 is just as good as that of the finer indicators η_p , $p \gg 2$ when employed in an adaptive mesh refinement algorithm. More generally, as in the previous works [22] and [23], the properties of the bulk mesh are seen to govern properties of the surface AFEM.

Local efficiency results in which elementwise error indicators are bounded up to higher order terms by the finite element error are important because they give theoretical justification for using such indicators to selectively refine mesh elements. We study the question of efficiency by a combination of computation and theory. In section 4.2 we provide a partial efficiency result (one that considers only the “volumetric” portion $h_T \|f_h + \Delta_{\Gamma_h} u_h\|_{L_2(T)}$ of the residual indicators) for the indicator η_2 that is slightly weaker than typical results for Euclidean domains. This estimate rests on a simple but fundamental observation that helps to explain why the properties of the outer mesh are inherited by the surface mesh: Even though a given surface triangle T may be irregular (anisotropic) or have diameter much smaller than that of the bulk tetrahedron from which it is inherited, there is always a surface element in a small patch surrounding T which is shape regular and “full size” (i.e., it has diameter equivalent to h_T).

The irregularity of the mesh prevents us from using standard tools to prove a corresponding result for the “jump” portion of the residual indicators, so we instead study their efficiency computationally. We found that when using the local error indicators resulting from the a posteriori estimate for adaptive mesh refinement, our local indicators indeed satisfy a local efficiency property very similar to the corresponding Euclidean property. Our numerical examples for a Laplace–Beltrami equation having solutions with point singularities also confirm the reliability of the error indicators for any $2 \leq p \leq \infty$. In addition, employing a simple refinement strategy provides optimal order convergence in the H^1 norm, and the choice of p in (1.2) has essentially no effect on the observed error decrease even with respect to constants. The latter observation

reinforces our assertion that properties of the bulk mesh govern the properties of the surface AFEM.

The remainder of the paper is organized as follows. Section 2 collects necessary preliminaries and assumptions. The surface FEM is defined here. In section 3 we define the local error indicator and prove the corresponding error bound (the reliability of the indicator). In section 4 we provide some brief theoretical comments on local efficiency properties of our error indicators. Numerical examples illustrating the efficiency of the entire approach are presented in section 5. Some closing remarks are given in section 6.

2. Preliminaries. In this section we make necessary assumptions on the properties of the surface Γ and its approximation and also introduce volume and surface finite element spaces and the FEM for (1.1). Furthermore we discuss the assumptions on triangulations required for our analysis. Finally, we recall some useful results from the theory of Sobolev spaces.

2.1. Geometry. We assume that Γ is a closed C^2 surface embedded in \mathbb{R}^3 . This implies the existence of a C^2 distance function $d : U \rightarrow \mathbb{R}$ such that $\Gamma = \{x \in U : d(x) = 0\}$. Here U is a tubular neighborhood about Γ of width δ ; more precisely $U = \{x \in \mathbb{R}^3 : \text{dist}(x, \Gamma) < \delta\}$, where δ is bounded by the reciprocal of the maximum over Γ of the moduli of all principal curvatures. We assume that d is negative inside of Γ and positive outside. Thus for $x \in U$, $\text{dist}(x, \Gamma) = |d(x)|$.

Under these conditions, there is an orthogonal projection $p : U \rightarrow \Gamma$ given by $p(x) = x - d(x)\nu(x)$, where $\nu(x) = \nabla d(x)$ is the unit outward normal for $x \in \Gamma$. Otherwise it defines the normal direction to Γ : $p(x)$ lies on Γ , and $x - p(x) = d(x)\nu(x)$ is orthogonal to the tangent plane to Γ at $p(x)$. Finally, let $\mathbf{H} = D^2d = \nabla\nu$ be the Weingarten map. More details of the present formalism can be found in [8, section 2.1].

2.2. Finite element mesh and spaces. The key feature of this paper is that the finite element discretization of (1.1) is defined relative to an “outer” triangulation, that is, a volume mesh. Let \mathcal{T} be a shape regular simplicial decomposition of a (three-dimensional) neighborhood of Γ ; we assume for notational simplicity that \mathcal{T} extends to \mathbb{R}^3 . We define the set of all tetrahedra intersecting the smooth surface Γ ,

$$\mathcal{T}_\Gamma = \bigcup_{S \in \mathcal{T}, S \cap \Gamma \neq \emptyset} \bar{S},$$

and require that $\mathcal{T}_\Gamma \subset U$. We additionally require that the mesh \mathcal{T} resolves Γ and U in a manner which is made more precise below. Also, denote by V_h the continuous piecewise linear functions on \mathcal{T} . Let $I_h : H^1(\mathbb{R}^3) \rightarrow V_h$ be the Scott–Zhang interpolation operator, and given $S \in \mathcal{T}$, let ω_S be the patch of tetrahedral elements touching S . We furthermore denote by ω'_S the patch of elements touching ω_S and by ω''_S the patch of elements touching ω'_S .

We now summarize standard properties of I_h which we will need in our arguments. In the lemma below and further on in the paper, we shall write $a \lesssim b$ when $a \leq Cb$ for a constant C depending possibly on the shape regularity of \mathcal{T} and geometric properties of Γ , but not on the local mesh size of \mathcal{T} .

LEMMA 2.1. *Assume that $u \in H^{3/2}(U)$. Then given $S \in \mathcal{T}$,*

$$(2.1) \quad \|u - I_h u\|_{L_2(S)} \lesssim h_T^{3/2} \|u\|_{H^{3/2}(\omega_S)}$$

and

$$(2.2) \quad \|u - I_h u\|_{H^1(S)} \lesssim h_T^{1/2} \|u\|_{H^{3/2}(\omega_S)}.$$

Above we have denoted by $H^{3/2}$ the standard fractional-order Sobolev norm. We give a precise definition below. The above approximation results are entirely standard except for the presence of a fractional-order Sobolev space. In the case of fractional-order Sobolev spaces one gets (2.1) and (2.2) from Theorem 5.1 of [?] (cf. section 6 and Remark 7.3 of [11]).

For computational purposes one needs a discrete approximation Γ_h of the smooth surface Γ . A distinct feature of the present approach is that no additional triangulation or meshing are required for building Γ_h . To this end, let $d_h : C(U) \rightarrow V_h$ be the piecewise linear Lagrange interpolant of the distance function d on the volume mesh \mathcal{T}_Γ . The computational surface Γ_h is defined to be the 0-level set of the approximate distance function d_h . Note that Γ_h is a closed W_∞^1 surface composed of a set of polygonal faces \mathcal{F} . Each face $T \in \mathcal{F}$ is the intersection of a plane with a tetrahedron $S \in \mathcal{T}$ and thus may be either a triangle or a quadrilateral. If T is a quadrilateral, then T is divided into two triangles, so without loss of generality we may assume that T is a triangle. Given $T \in \mathcal{F}$, let S_T be the tetrahedron containing T , and let $h_T = \text{diam}(S_T)$. Further, we define the set of all tetrahedra intersecting the discrete surface Γ_h :

$$\mathcal{T}_{\Gamma_h} = \bigcup_{S \in \mathcal{T}: S \cap \Gamma_h \neq \emptyset} \bar{S}.$$

Note that $\mathcal{T}_{\Gamma_h} \subset \mathcal{T}_\Gamma$ since $S \cap \Gamma_h \neq \emptyset$ implies that d_h and thus d changes sign on S . However, in general $\mathcal{T}_{\Gamma_h} \neq \mathcal{T}_\Gamma$, since d may change sign on S without d_h doing so.

Remark 1. More generally, Γ_h may be a polygonal approximation to Γ consistent with the volume triangulation \mathcal{T} (cf. [22]). Moreover, in some applications Γ may not be known at all, and Γ_h may, for example, be taken to be the 0-level of a discrete function solving a discrete level set equation on a volume mesh.

2.3. Surface FEM. The key surface finite element space is V_h^Γ , the space of functions obtained by restricting functions in V_h to Γ_h . Then the surface FEM introduced in [22] reads as follows: Find the finite element solution $u_h \in V_h^\Gamma$ satisfying

$$(2.3) \quad \int_{\Gamma_h} \nabla_{\Gamma_h} u_h \nabla_{\Gamma_h} v_h \, ds_h = \int_{\Gamma_h} f_h v_h \, ds_h \quad \forall v_h \in V_h^\Gamma.$$

Here f_h is an approximation to f defined on Γ_h , and we require the side conditions $\int_{\Gamma_h} u_h \, ds_h = \int_{\Gamma_h} f_h \, ds_h = 0$ in order to ensure existence and uniqueness of solutions to (2.3). Note that although the method (2.3) employs the outer (volume) finite element space V_h (through its trace V_h^Γ on Γ_h), only nodal values of functions in V_h corresponding to nodes lying adjacent to Γ_h contributed to V_h^Γ . Thus, the size of the resulting linear algebraic system essentially corresponds to the two-dimensional nature of the original problem (1.1).

Two facts complicate the analysis of the FEM in (2.3). First, even though \mathcal{T} is shape regular, the surface triangulation \mathcal{F} may contain triangles with arbitrarily small angles. Second, it is possible that $\text{diam}(T) \ll h_T$ even if T is shape regular. Because of these facts, we always seek to apply approximation results on the *volume* mesh \mathcal{T} and not on the surface mesh \mathcal{F} .

The following result for the error of the method (2.3) is known [22]. Assume for a moment that the volume mesh is quasi-uniform and $\max_{S \in \mathcal{T}} \text{diam}(S) \leq h$. Let $u \in H^2(\Gamma)$ be the weak solution of (1.1) and $u_h \in V_h^\Gamma$ the solution of (2.3) with $f_h = f^e - c_f$, where c_f is such that $\int_{\Gamma_h} f_h \, ds = 0$; then it holds that

$$(2.4) \quad \|u^e - u_h\|_{L^2(\Gamma_h)} + h \|\nabla_{\Gamma_h}(u^e - u_h)\|_{L^2(\Gamma_h)} \leq ch^2 \|f\|_{L^2(\Gamma)},$$

where the constant c is independent of f and h and u^e is the extension of u from Γ as defined in the next paragraph. Thus for a quasi-uniform volume mesh the error estimate for the surface FEM resembles the standard result for the usual Courant finite elements. In the present paper we are *not* assuming the quasi-uniformity property and allow the volume meshes to be locally refined.

2.4. Correspondence between Γ and Γ_h . In this section we briefly record notation and facts that will allow us to easily transfer quantities between the surfaces Γ and Γ_h . We refer to [8] for more details regarding both the definitions we make here and practical computation of various geometric quantities. First, we will routinely use lifts and extensions of functions. Given $\psi \in H^1(\Gamma)$, we denote by $\psi^e \in H^1(U)$ its extension from Γ along normals, i.e., the function defined by $\psi^e(x) = \psi(p(x))$; ψ^e is constant in the direction normal to Γ . Given $\psi_h \in H^1(\Gamma_h)$, $x \in \Gamma_h$, and $p(x) \in \Gamma$, we let $\psi_h^\ell(p(x)) = \psi_h(x)$ be the lift of ψ_h to Γ .

Given $x \in \Gamma$, let $\mathbf{P} = \mathbf{I} - \nu(x) \otimes \nu(x)$ be the projection onto the tangent plane to Γ at x . Note that ν , and thus \mathbf{P} , is constant in U in the direction normal to Γ . Similarly, given $x \in \Gamma_h$, we let $\mathbf{P}_h(x) = \mathbf{I} - \nu_h(x) \otimes \nu_h(x)$ be the projection onto the tangent plane to Γ_h at x ; here ν_h is the outward-pointing normal to Γ_h .

Let ds and ds_h denote surface measure on Γ and Γ_h , respectively. We then define μ_h to be the ratio of these measures or, more precisely, for $x \in \Gamma_h$ we have $\mu_h(x) ds_h(x) = ds(p(x))$. Then $\int_\Gamma v(x) ds = \int_{\Gamma_h} v^e(x) \mu_h(x) ds_h$, and $\int_{\Gamma_h} v_h(x) ds_h = \int_\Gamma v_h^\ell(x) \frac{1}{\mu_h(x)} ds$. We also define the transfer operator \mathbf{A}_h for the Dirichlet form by $\mathbf{A}_h(x) = \mathbf{A}_h^\ell(p(x)) = \frac{1}{\mu_h(x)} [\mathbf{P}(x)][(\mathbf{I} - d\mathbf{H})(x)][\mathbf{P}_h(x)][(\mathbf{I} - d\mathbf{H})(x)][\mathbf{P}(x)]$. Then $\int_{\Gamma_h} \nabla_{\Gamma_h} v_h \nabla_{\Gamma_h} \psi_h ds_h = \int_\Gamma \mathbf{A}_h^\ell \nabla_\Gamma v_h^\ell \nabla_\Gamma \psi_h^\ell ds$.

2.5. A mesh restriction. We first introduce further notation. A tetrahedron $S \in \mathcal{T}$ in the outer (also called bulk or volume) triangulation may or may not correspond to a flat surface element $T \in \mathcal{F}$. Given $S \in \mathcal{T}$, we let $\tilde{T}_S = S \cap \Gamma$ be the *curved* “element” intersecting S . Recall that for the discrete surface element $T \in \mathcal{F}$ the corresponding volume element is denoted by S_T . We shall denote by \tilde{T} the intersection of S_T with Γ , that is, $\tilde{T} = \tilde{T}_{S_T}$. Note carefully that \tilde{T}_S may be nonempty even if S does not contain any flat surface element lying in \mathcal{F} and that given $T \in \mathcal{F}$ it is generally true that $p(T) \neq \tilde{T}$.

In our proofs below we will apply approximation results for *curved* surface elements \tilde{T} , that is, error estimates for the difference between functions on \tilde{T} and the restriction of polynomials defined on S_T to \tilde{T} . In contrast, the natural residual equations for our surface FEM involve comparing polynomials on *flat* elements T with the extension ψ^e of $\psi \in H^1(\Gamma)$. We shall have to account for this difference in our estimates, which becomes somewhat technical because as noted above there is not an a priori guarantee that $p(T) \subset S_T$. In order to control the number of volume elements that $p(T)$ can touch, we make the following assumption.

Assumption 1. For a discrete surface element $T \in \mathcal{F}$, let $\Omega_T = \{y : y = tx + (1 - t)p(x) \text{ for some } 0 \leq t \leq 1, x \in T\}$. That is, Ω_T is the set of all points that lie on a line segment connecting some point $x \in T$ and its image $p(x) \in \Gamma$. We assume that

$$(2.5) \quad \Omega_T \subset \omega_{S_T}.$$

We will also need the following similar assumption.

Assumption 2. Let \mathbb{P} be the plane containing a given surface element $T \in \mathcal{F}$. Then

$$(2.6) \quad p(\omega_{S_T} \cap \mathbb{P}) \subset \omega'_{S_T}.$$

Assumptions 1 and 2 are always satisfied if Γ is sufficiently resolved by the outer triangulation. To verify this assertion for Assumption 1, note that Ω_T consists of points lying a distance no more than $c_1 h_T^2$ from T for some $c_1 > 0$, since for $x \in \mathcal{T}$ we have $|d(x)| = |d(x) - d_h(x)| \leq c_1 h_T^2$ by standard properties of the Lagrange interpolant. On the other hand, shape regularity of \mathcal{T} implies local quasi-uniformity of \mathcal{T} , which in turn implies that the patch ω_{S_T} contains all points lying a distance at most $C_2 h_T$ from T for some $C_2 > 0$. Here C_2 depends on shape regularity properties of the outer triangulation. Thus Assumption 1 is satisfied when $c_1 h_T^2 \leq C_2 h_T$, i.e., when $h_T \leq \frac{C_2}{c_1}$. Note that $\frac{C_2}{c_1}$ depends on geometric properties of Γ , properties of the Lagrange interpolant, and the shape regularity of \mathcal{T} . We do not attempt to bound $\frac{c_1}{C_2}$, though it should in principle be possible to do. One could also check this assumption in practice if desired without too great of difficulty. A similar argument holds for Assumption 2 after noting that by standard properties of the Lagrange interpolant $|d(x)| \leq \tilde{c}_1 h_T^2$ for $x \in \mathbb{P} \cap \omega_{S_T}$.

We now state an elementary lemma which gives a bound for the difference between the restriction of finite element functions $\psi_h \in V_h$ to Γ_h (that is, $\psi_h|_{\Gamma_h}$) and their extensions from Γ to Γ_h (that is, $\psi_h^e|_{\Gamma_h}$). Note that below we bound the pointwise quantity $|\psi_h(x) - \psi_h^e(x)|$ defined on the surface Γ_h by an L_2 term over the volume patch ω_{S_T} .

LEMMA 2.2. *Let $\psi_h \in V_h$ and $T \in \mathcal{F}$. Then for $x \in \bar{T}$,*

$$(2.7) \quad |\psi_h(x) - \psi_h^e(x)| \lesssim h_T^{1/2} \|\nabla \psi_h\|_{L_2(\omega_{S_T})}.$$

Proof. Let $T \in \mathcal{F}$. Let also $g(t) = \psi_h(tx + (1-t)p(x))$, $0 \leq t \leq 1$, so that $g(0) = \psi_h(p(x))$ and $g(1) = \psi_h(x)$. Noting that for $x \notin \Gamma$ $\nu(x) = \frac{1}{d(x)}(p(x) - x)$ and thus $g'(t) = \nabla \psi_h(tx + (1-t)p(x)) \cdot (x - p(x)) = -d(x) \nabla \psi_h(tx + (1-t)p(x)) \cdot \nu(x)$, we have for any $x \in \bar{T}$

$$\begin{aligned} |\psi_h(x) - \psi_h^e(x)| &= |\psi_h(x) - \psi_h(p(x))| = |g(0) - g(1)| = \left| \int_0^1 g'(t) dt \right| \\ &= \left| d(x) \int_0^1 \nabla \psi_h(tx + (1-t)p(x)) \cdot \nu(x) dt \right| \\ &\lesssim |d(x)| \|\nabla \psi_h\|_{L_\infty(\Omega_T)}. \end{aligned}$$

Using Assumption 1 and recalling that $|d(x)| \leq Ch_T^2$ for $x \in \bar{T}$, noting that $h_T \simeq h_{T'}$ for $T' \subset \omega_{S_T}$ by shape regularity of \mathcal{T} , and employing an inverse estimate, we proceed:

$$(2.8) \quad |\psi_h(x) - \psi_h^e(x)| \leq Ch_T^2 \|\nabla \psi_h\|_{L_\infty(\bar{\omega}_{S_T})} \leq Ch_T^{1/2} \|\nabla \psi_h\|_{L_2(\omega_{S_T})} \quad \forall x \in \bar{T}. \quad \square$$

2.6. Sobolev spaces, extensions, and imbeddings. In [22] a priori error estimates for the surface FEM defined above were proved assuming quasi-uniform volume meshes. An important tool in this analysis was the use of the canonical extension u^e of the solution to elliptic PDE from smooth surface, i.e., the extension which is constant in the normal direction. One major technical difficulty with extending the techniques of [22] for the case of a posteriori estimates is that local approximation estimates from [22] (see, e.g., (3.26) on p. 3343) involve on the right-hand side a norm of a function over the normal projection onto the smooth surface Γ of a volume element intersecting Γ . If the outer tetrahedrons are quasi-uniform, then there is finite overlap of such projections over all tetrahedron intersecting the surface, so these local norms on the right-hand of an inequality sum up to a global norm. However, if one

allows the tetrahedrons to be refined adaptively to a point or a line on the smooth surface, then it is impossible to show a uniform bound on the number of the outer tetrahedrons whose projections onto Γ have nonempty overlap. Therefore “generic” constants on the right-hand side may depend on the refinement level. Since we want our a posteriori estimates to remain useful in the adaptive case, we take an approach different from [22]. The new approach relies on an extension operator from $H^1(\Gamma)$ to $H^{3/2}(\mathbb{R}^3)$.

Next we recall fractional-order Sobolev spaces. Given a subdomain Ω of \mathbb{R}^n , and $1 \leq p < \infty$, we let $W_p^s(\Omega)$ be the standard Sobolev space having L_p index p and smoothness index s when s is a nonnegative integer. In the general case, let $s = \bar{s} + \theta$, where \bar{s} is an integer and $0 < \theta < 1$. We then define the seminorm

$$(2.9) \quad |u|_{W_p^s(\Omega)}^p = \sum_{|\alpha|=\bar{s}} \iint_{\Omega \times \Omega} \frac{|D^\alpha u(x) - D^\alpha u(y)|^p}{|x - y|^{n+\theta p}} dx dy$$

and the norm

$$(2.10) \quad \|u\|_{W_p^s(\Omega)} = \left(\|u\|_{W_p^{\bar{s}}(\Omega)}^p + |u|_{W_p^s(\Omega)}^p \right)^{1/p};$$

cf. [18, Definition 1.3.2.1]. We will use the above definitions with $p = 2$ only, and accordingly set $H^s(\Omega) = W_2^s(\Omega)$.

We now state the following important lemma.

LEMMA 2.3. *Let Γ be a C^2 surface as above. Then given $\psi \in H^1(\Gamma)$, there exists $\tilde{\psi} \in H^{3/2}(\mathbb{R}^3)$ such that*

$$(2.11) \quad \|\tilde{\psi}\|_{H^{3/2}(\mathbb{R}^3)} \lesssim \|\psi\|_{H^1(\Gamma)}, \quad \tilde{\psi}|_\Gamma = \psi.$$

Proof. Take $\tilde{\psi}$ to be the harmonic extension of ψ from Γ to \mathbb{R}^3 . The desired result is stated in [20, p. 198]. \square

Below ψ will generally be fixed, and we shall denote by ψ both an H^1 function on Γ and its bounded $H^{3/2}$ extension to \mathbb{R}^3 .

Remark 2. The a posteriori error analysis below could be substantially simplified if we could prove the uniform boundedness over a whole family of surfaces $\{\Gamma_h\}$ of the corresponding $H^{3/2}$ extension operators. In particular, let \mathcal{T}_0 be an initial volume mesh, and let Γ_0 be the corresponding discrete surface approximation. Also let \mathbb{T} be the set of all shape regular meshes that can be derived by systematic refinement (e.g., newest-vertex bisection) of \mathcal{T}_0 , and let $\Gamma_\mathbb{T}$ be the corresponding family of discrete approximations of Γ . It is reasonable to conjecture that $\Gamma_\mathbb{T}$ is a uniform family of approximations to Γ in the Lipschitz norm (though we do not prove this), and the bounded extension result (2.11) only requires that Γ be Lipschitz. Thus we conjecture that the constant in (2.11) is in fact uniformly bounded over $\Gamma_\mathbb{T}$. If this conjecture is true, one can (i) avoid entirely two flattening arguments that we employ below and also thereby avoid the assumptions (2.5) and (2.6) above on the resolution of Γ by the mesh \mathcal{T} , and (ii) avoid using larger patches of elements; cf. the definition of ω'_S and ω''_S in section 2.2. However, proving (2.11) uniformly over $\Gamma_\mathbb{T}$ would involve proving several nontrivial results from harmonic analysis also with uniform constants, and we do not pursue such a uniform bound.

Next we state Sobolev imbedding and trace results. We first state an imbedding result that will allow us to trace the dependence of imbedding constants on an integrability index p . This result is fairly standard for $n = 2$ and can be derived, for

example, from [16, p. 158]. For fractional-order spaces ($n = 1$), the result can be found in [21].

LEMMA 2.4. *Let $2 \leq p < \infty$, and assume that $u \in H_0^{n/2}(\mathbb{R}^n)$, $n = 1, 2$. Then*

$$(2.12) \quad \|u\|_{L_p(\mathbb{R}^n)} \lesssim \sqrt{p} |u|_{H^{n/2}(\mathbb{R}^n)}.$$

We next state trace results; the lemma below contains special cases of [2, Theorem 7.58].

LEMMA 2.5. *Let $s > 0$ and $1 \leq k \leq n$. Then if $u \in H^{s+(n-k)/2}(\mathbb{R}^n)$,*

$$(2.13) \quad \|u\|_{H^s(\mathbb{R}^k)} \lesssim \|u\|_{H^{s+(n-k)/2}(\mathbb{R}^n)}.$$

Finally we state extension results. The result below is found, for example, in Theorem 1.4.3.1 of [18]. (Note that the unit simplex has uniformly Lipschitz boundary.)

LEMMA 2.6. *Let \hat{K} be the unit simplex in \mathbb{R}^n , $n = 2, 3$. Then there exists an extension operator $E : H^s(\hat{K}) \rightarrow H^s(\mathbb{R}^n)$ such that*

$$(2.14) \quad \|Ev\|_{H^s(\mathbb{R}^n)} \lesssim \|v\|_{H^s(\hat{K})}, \quad s = 1, \frac{3}{2}, \quad v \in H^s(\hat{K}).$$

3. A posteriori error estimate.

3.1. Error indicators. The basic philosophy of the error analysis of the surface FEM studied here is to employ approximation properties on the outer triangulation. From this standpoint, it appears natural to consider an error indicator

$$(3.1) \quad \eta_2(T) = h_T \|f_h + \Delta_{\Gamma_h} u_h\|_{L_2(T)} + h_T^{1/2} \|[\![\nabla_{\Gamma_h} u_h]\!] \|_{L_2(\partial T)}$$

and corresponding error estimator $(\sum_{T \in \mathcal{F}} \eta_2(T)^2)^{1/2}$ for the energy norm. As we show below, this estimator reliably estimates the energy error up to geometric terms, and numerical tests also indicate that it possesses a certain local efficiency property.

Since the discrete surface Γ_h may intersect the outer triangulation in an arbitrary way, a surface element edge length $|e|$ and area $|T|$ are sometimes much smaller than h_T and h_T^2 , respectively. We seek to take this fact into account in our estimator in the sharpest fashion possible. Given $p \in [2, \infty]$, we thus define the error estimator

$$(3.2) \quad \eta_p = C_p \left(|T|^{1/2-1/p} h_T^{2/p} \|f_h + \Delta_{\Gamma_h} u_h\|_{L_2(T)} + \sum_{e \subset \partial T} |e|^{1/2-1/p} h_T^{1/p} \|[\![\nabla_{\Gamma_h} u_h]\!] \|_{L_2(e)} \right).$$

Taking $p = 2$, we see that η_2 in (3.1) and (3.2) coincide up to a constant factor. At the same time, it would be desirable to consider the other extreme case of $p = \infty$. However, proving reliability of the resulting error estimator

$$(3.3) \quad \left(\sum_{T \in \mathcal{F}} |T| \|f_h + \Delta_{\Gamma_h} u_h\|_{L_2(T)}^2 + \sum_{e \subset \partial T} |e| \|[\![\nabla_{\Gamma_h} u_h]\!] \|_{L_2(e)}^2 \right)^{1/2}$$

using our techniques below would require that certain limit cases of Sobolev embeddings hold. They do not, as, for example, (2.12) demonstrates. Stated differently, in our arguments C_p blows up as $p \rightarrow \infty$. Thus although numerical experiments suggest

that $p = \infty$ remains a reasonable choice, we are unable to prove that the estimator in (3.3) is reliable, so in the analysis below we always assume $p \in [2, \infty)$.

Remark 3. An even finer estimator can be derived by noting that p may be chosen differently on each element T and on each edge e and that from (2.12) we have $C_p = \sqrt{p}$. Let $T \in \mathcal{F}$ have edges each of which is denoted by e , and let $p_T, p_e \in [2, \infty]$, where again p_e may be different for each edge of T . Letting \tilde{p} be the vector consisting of p_T and the p_e , we then define the elementwise error indicator

$$(3.4) \quad \begin{aligned} \eta_{\tilde{p}}(T) &= \sqrt{p_T}|T|^{1/2-1/p_T} h_T^{2/p_T} \|f_h + \Delta_{\Gamma_h} u_h\|_{L_2(T)} \\ &+ \sum_{e \subset \partial T} \sqrt{p_e}|e|^{1/2-1/p_e} h_T^{1/p_e} \|[\nabla_{\Gamma_h} u_h]\|_{L_2(e)}. \end{aligned}$$

Seeking values of p_T and p_e which minimize $\eta_{\tilde{p}}(T)$ yields $p_T = \max\{2, 2 \ln(h_T^2/|T|)\}$ and $p_e = \max\{2, 2 \ln(h_T/|e|)\}$.

In order to keep notation manageable we will prove up to geometric terms the reliability of the H^1 error estimator $(\sum_{T \in \mathcal{F}} \eta_p^2(T))^{1/2}$, where p has a fixed value in $[2, \infty)$ and $C_p = \sqrt{p}$. It will be clear from our proofs, however, that p may be chosen independently on each element T and face e . We do not treat the more complicated case (3.4) separately or otherwise consider it further.

3.2. Statement of results. We now state our main theoretical result giving reliability up to geometric terms of estimators derived from our error indicators.

THEOREM 3.1. *Suppose that Γ is a closed, compact C^2 surface embedded in \mathbb{R}^3 as in section 2.1 and that all assumptions concerning the finite element mesh in sections 2.4 and 2.5 are satisfied. Let u and u_h be the solutions to (1.1) and (2.3), respectively. Then for $p \in [2, \infty)$*

$$(3.5) \quad \begin{aligned} \|\nabla_{\Gamma}(u - u_h^{\ell})\|_{L_2(\Gamma)} &\leq C_1 \left(\sum_{T \in \mathcal{F}} \eta_p(T)^2 \right)^{1/2} \\ &+ \|\mathbf{B}_h \nabla_{\Gamma_h} u_h\|_{L_2(\Gamma_h)} + C_2 \|\sqrt{\mu_h} f^e - f_h / \sqrt{\mu_h}\|_{L_2(\Gamma_h)}. \end{aligned}$$

Here C_1 depends on the shape regularity of the outer mesh \mathcal{T} and the geometric properties of Γ , $\mathbf{B}_h = \sqrt{\mu_h}[\mathbf{P} - \mathbf{A}_h][\mathbf{I} - d\mathbf{H}]^{-1}[\mathbf{I} - (\nu_h \otimes \nu) / (\nu_h \cdot \nu)]$, and C_2 is the Poincaré constant for Γ , i.e., $\|\psi\|_{L_2(\Gamma)} \leq C_2 \|\nabla_{\Gamma} \psi\|_{L_2(\Gamma)}$ when $\int_{\Gamma} \psi \, ds = 0$.

We now briefly compare our results with those in [8], where a posteriori estimates for FEM based on shape-regular surface triangulations were proved. First, the constants corresponding to C_1 in [8] are locally defined, and their dependence on geometric properties of Γ is computed explicitly. While C_1 here depends on roughly the same quantities as the corresponding constants in [8], its dependence on geometry is much more complicated (depending, for example, on the constant hidden in the $H^{3/2}$ extension inequality (2.11)), and we do not attempt to trace it.

The last two terms in (3.5) control the error induced by discretizing Γ and are essentially the same as the corresponding terms encountered in [8]. $\|\mathbf{B}_h \nabla_{\Gamma_h} u_h\|_{L_2(\Gamma_h)}$ is of higher order ($O(h^2)$ in an a priori sense), and the operator \mathbf{B}_h explicitly and locally measures dependence on geometry. The term $\|\sqrt{\mu_h} f^e - f_h / \sqrt{\mu_h}\|_{L_2(\Gamma_h)}$ measures the deviation of f_h from f^e in an appropriate sense; in particular we see that taking $f_h = \mu_h f^e$ eliminates this term. Note also that $|1 - \mu_h| \lesssim h^2$, so that taking $f_h = f^e$ also results in this term being of higher order. It should also be noted that the fact that the geometric terms are of higher order in h_T is not affected by the lack of regularity of the surface mesh, since the order of the corresponding geometric

properties is determined by the error $d - d_h$ in the Lagrange interpolant of d on the *outer* mesh. Because of the nearly complete correspondence of these terms with the similar terms in [8], we do not study them in any further detail below.

3.3. Residual equation. Consider the surface finite element error $e_h = u^e - u_h$ on Γ_h . In our analysis we prove an a posteriori bound for the lift of e_h on Γ , i.e., $e_h^\ell = u - u_h^\ell$ on Γ . Recalling that

$$(3.6) \quad \|\nabla_\Gamma e_h^\ell\|_{L_2(\Gamma)} = \sup_{\psi: \int_\Gamma \psi = 0} \|\nabla_\Gamma \psi\|_{L_2(\Gamma)} = 1 \int_\Gamma \nabla_\Gamma e_h^\ell \nabla_\Gamma \psi \, ds,$$

we let $\psi \in H^1(\Gamma)$ with $\|\nabla_\Gamma \psi\|_{L_2(\Gamma)} = 1$, $\int_\Gamma \psi \, ds = 0$, and then find as in (3.3.5) of [8] that for any $\psi_h \in V_h^\Gamma$ it holds that

$$(3.7) \quad \begin{aligned} \int_\Gamma \nabla_\Gamma e_h^\ell \nabla_\Gamma \psi \, ds &= \int_{\Gamma_h} (f_h + \Delta_{\Gamma_h} u_h)(\psi^e - \psi_h) \, ds_h \\ &\quad - \frac{1}{2} \sum_{T \in \mathcal{F}} \int_{\partial T} \llbracket \nabla_{\Gamma_h} u_h \rrbracket (\psi^e - \psi_h) \, dr \\ &\quad - \int_\Gamma [\mathbf{P} - \mathbf{A}_h^\ell] \nabla_\Gamma u_h^\ell \nabla_\Gamma \psi \, ds + \int_{\Gamma_h} (f^e \mu_h - f_h) \psi^e \, ds_h. \end{aligned}$$

In the above, let e be an edge shared by elements T_1 and T_2 which have normals \vec{n}_1 and \vec{n}_2 , respectively. Then $\llbracket \nabla_{\Gamma_h} u_h \rrbracket = \nabla_{\Gamma_h} u_h|_{T_1} \cdot \vec{n}_1 - \nabla_{\Gamma_h} u_h|_{T_2} \cdot \vec{n}_2$ is the jump in the normal derivative across e .

We now fix p with $2 \leq p < \infty$ and let q be the conjugate index satisfying $\frac{1}{p} + \frac{1}{q} = 1$. Since it should not cause confusion we also denote by ψ the $H^{3/2}$ extension of ψ to \mathbb{R}^3 given by Lemma 2.3. Further, we take $\psi_h = I_h \psi$ in (3.7). Using Hölder’s inequality ($\|f_h + \Delta_{\Gamma_h} u_h\|_{L_q(T)} \lesssim |T|^{1/2-1/p} \|f_h + \Delta_{\Gamma_h} u_h\|_{L_2(T)}$, and $\|\llbracket \nabla_{\Gamma_h} u_h \rrbracket\|_{L_q(e)} \lesssim |e|^{1/2-1/q} \|\llbracket \nabla_{\Gamma_h} u_h \rrbracket\|_{L_2(e)}$), we compute

$$(3.8) \quad \begin{aligned} &\int_{\Gamma_h} (f_h + \Delta u_h)(\psi^e - I_h \psi) \, ds_h - \frac{1}{2} \sum_{T \in \mathcal{F}} \int_{\partial T} \llbracket \nabla_{\Gamma_h} u_h \rrbracket (\psi^e - I_h \psi) \, dr \\ &\lesssim \sum_{T \in \mathcal{F}} \left[\|f_h + \Delta u_h\|_{L_q(T)} \|\psi^e - I_h \psi\|_{L_p(T)} \right. \\ &\quad \left. + \sum_{e \subset \partial T} \|\llbracket \nabla_{\Gamma_h} u_h \rrbracket\|_{L_q(e)} \|\psi^e - I_h \psi\|_{L_p(e)} \right] \\ &\lesssim \sum_{T \in \mathcal{F}} \eta_p(T) p^{-1/2} \left(h_T^{-2/p} \|\psi^e - I_h \psi\|_{L_p(T)} + \sum_{e \subset \partial T} h_T^{-1/p} \|\psi^e - I_h \psi\|_{L_p(e)} \right) \\ &\lesssim \left(\sum_{T \in \mathcal{F}} \eta_p(T)^2 \right)^{1/2} \left(p^{-1} \sum_{T \in \mathcal{F}} \left[h_T^{-4/p} \|\psi^e - I_h \psi\|_{L_p(T)}^2 \right. \right. \\ &\quad \left. \left. + \sum_{e \subset \partial T} h_T^{-2/p} \|\psi^e - I_h \psi\|_{L_p(e)}^2 \right] \right)^{1/2}. \end{aligned}$$

The volume term $\|\psi^e - I_h \psi\|_{L_p(T)}$ and the edge terms $\|\psi^e - I_h \psi\|_{L_p(e)}$ on the right-hand side of (3.8) are treated separately below.

3.4. Bounding the volume term. We first bound the term $p^{-1}h_T^{-4/p}\|\psi^e - I_h\psi\|_{L_p(T)}^2$. Using (2.7) and noting that $|T| \leq Ch_T^2$, we compute

$$\begin{aligned}
 & h_T^{-2/p}\|\psi^e - I_h\psi\|_{L_p(T)} \\
 & \lesssim h_T^{-2/p}(\|\psi^e - (I_h\psi)^e\|_{L_p(T)} + \|(I_h\psi)^e - I_h\psi\|_{L_p(T)}) \\
 (3.9) \quad & \lesssim h_T^{-2/p}(\|\psi^e - (I_h\psi)^e\|_{L_p(T)} + |T|^{1/p}\|(I_h\psi)^e - I_h\psi\|_{L_\infty(T)}) \\
 & \lesssim h_T^{-2/p}\|\psi^e - (I_h\psi)^e\|_{L_p(T)} + \|(I_h\psi)^e - I_h\psi\|_{L_\infty(T)} \\
 & \lesssim h_T^{-2/p}\|\psi^e - (I_h\psi)^e\|_{L_p(T)} + h_T^{1/2}\|\nabla(I_h\psi)\|_{L_2(\omega_{S_T})}.
 \end{aligned}$$

Here $(I_h\psi)^e$ denotes the extension of the trace of $I_h\psi$ on Γ , that is, $(I_h\psi)^e = ([I_h\psi]_\Gamma)^e$. In order to bound the term $h_T^{-2/p}\|\psi^e - (I_h\psi)^e\|_{L_p(T)}$, we write $\rho = \psi - I_h\psi$ and use (2.5) in order to find that

$$(3.10) \quad \|\psi^e - (I_h\psi)^e\|_{L_p(T)} = \|\rho^e\|_{L_p(T)} \lesssim \|\rho\|_{L_p(p(T))} \leq \sum_{S \in \omega_{S_T}} \|\rho\|_{L_p(\tilde{T}_S)}.$$

Next we define a reference mapping which flattens \tilde{T}_S for a given element $S \in \mathcal{T}$. Fixing $S \in \mathcal{T}$ and letting \hat{K} be the reference unit simplex in \mathbb{R}^3 as above, let $\varphi : \hat{K} \rightarrow S$ be an affine mapping with $\|\nabla\varphi\| \lesssim h_T$ and $\|(\nabla\varphi)^{-1}\| \lesssim h_T^{-1}$. Such a mapping exists because of the shape regularity of the outer triangulation. We next recall that because Γ is a C^2 surface, there exists a C^2 chart $\tilde{\Phi}$ with uniformly bounded derivatives and for which $\tilde{\Phi}^{-1}$ has uniformly bounded derivatives, which maps an $O(1)$ -neighborhood N of \tilde{T}_S in \mathbb{R}^3 to \mathbb{R}^3 and which has the property that $\Gamma \cap N$ lies in a plane. It is not difficult to extend $\tilde{\Phi}$ to all of \mathbb{R}^3 so that the resulting extension has bounded derivatives, has a bounded inverse, and flattens an $O(1)$ -neighborhood of \tilde{T}_S . We then define a corresponding flattening map for the reference space by $\Phi = \varphi^{-1} \circ \tilde{\Phi} \circ \varphi$. It is easy to check that then Φ and Φ^{-1} are also uniformly bounded in C^2 and $\Phi(\varphi^{-1}(\tilde{T}_S))$ is flat.

Define $\hat{\rho}$ on \hat{K} by $\hat{\rho} = \rho \circ \varphi$. Let also μ be a cutoff function which is 1 on a neighborhood of \hat{K} and 0 outside of a fixed ball about \hat{K} and which is uniformly bounded in C^2 . Given $S \in \mathcal{T}$ and recalling the definition of the extension operator E from Lemma 2.6 and preceding, we then compute

$$\begin{aligned}
 (3.11) \quad & h_T^{-2/p}\|\rho\|_{L_p(\tilde{T}_S)} \lesssim \|\hat{\rho}\|_{L_p(\varphi^{-1}(\tilde{T}_S))} \\
 & = \|E\hat{\rho}\|_{L_p(\varphi^{-1}(\tilde{T}_S))} \\
 & \lesssim \|E\hat{\rho} \circ \Phi^{-1}\|_{L_p(\Phi(\varphi^{-1}(\tilde{T}_S)))} \\
 & \lesssim \|\mu(E\hat{\rho} \circ \Phi^{-1})\|_{L_p(\mathbb{P})}.
 \end{aligned}$$

Here \mathbb{P} is a plane in \mathbb{R}^3 containing the flattened surface element $\Phi(\varphi^{-1}(\tilde{T}_S))$. Next we apply (2.12) with p as above and $n = 2$ and then apply (2.13) with $k = 2$, $n = 3$, and $s = 1$ (so that $s + (n - k)/2 = 3/2$). Using the smoothness of Φ and η , and recalling

from Lemma 2.6 that E is a bounded extension operator, we thus compute that

$$\begin{aligned}
 \|\mu(E\widehat{\rho} \circ \Phi^{-1})\|_{L_p(\mathbb{P})} &\lesssim \sqrt{p}\|\mu(E\widehat{\rho} \circ \Phi^{-1})\|_{H^1(\mathbb{P})} \\
 &\lesssim \sqrt{p}\|E\widehat{\rho} \circ \Phi^{-1}\|_{H^1(\mathbb{P})} \\
 (3.12) \qquad &\lesssim \sqrt{p}\|E\widehat{\rho} \circ \Phi^{-1}\|_{H^{3/2}(\mathbb{R}^3)} \\
 &\lesssim \sqrt{p}\|E\widehat{\rho}\|_{H^{3/2}(\mathbb{R}^3)} \\
 &\lesssim \sqrt{p}\|\widehat{\rho}\|_{H^{3/2}(\widehat{K})}.
 \end{aligned}$$

Noting that $\nabla \widehat{I_h \psi}$ is constant on the reference element \widehat{K} , we find that $\|\widehat{\rho}\|_{H^{3/2}(\widehat{K})} = \|\widehat{\psi} - \widehat{I_h \psi}\|_{H^1(\widehat{K})} + |\widehat{\psi}|_{H^{3/2}(\widehat{K})}$. Applying a scaling argument and then employing (2.1) and (2.2) yields

$$\begin{aligned}
 \|\widehat{\rho}\|_{H^{3/2}(\widehat{K})} &\lesssim h_T^{-3/2}\|\psi - I_h \psi\|_{L_2(S)} + h_T^{-1/2}\|\nabla(\psi - I_h \psi)\|_{L_2(S)} \\
 (3.13) \qquad &\quad + \|\psi\|_{H^{3/2}(\omega_S)} \\
 &\lesssim \|\psi\|_{H^{3/2}(\omega_S)}.
 \end{aligned}$$

Carrying out a similar argument for each $S \in \omega_{S_T}$ and collecting the resulting bounds (3.13), (3.12), and (3.11) into (3.10) yields

$$(3.14) \qquad h_T^{-2/p}\|\psi^e - (I_h \psi)^e\|_{L_p(T)} \lesssim \sqrt{p}\|\psi\|_{H^{3/2}(\omega'_{S_T})}.$$

Noting from (2.2) and the fact that $h_T \lesssim 1$ that $h_T^{1/2}\|\nabla(I_h \psi)\|_{L_2(\omega_{S_T})} \lesssim \|\nabla \psi\|_{L_2(\omega'_{S_T})}$, we finally insert this inequality and (3.14) into (3.9) in order to obtain

$$(3.15) \qquad p^{-1/2}h_T^{-2/p}\|\psi^e - I_h \psi\|_{L_p(T)} \lesssim \|\psi\|_{H^{3/2}(\omega'_{S_T})}.$$

Exploiting finite overlap of the patches ω'_{S_T} and using (2.11), we finally obtain

$$\begin{aligned}
 (3.16) \qquad \sum_{T \in \mathcal{F}} p^{-1}h_T^{-4/p}\|\psi^e - I_h \psi\|_{L_p(T)}^2 &\lesssim \|\psi\|_{H^{3/2}(\mathbb{R}^3)}^2 \lesssim \|\psi\|_{H^1(\Gamma)}^2 \\
 &\lesssim \|\nabla_{\Gamma} \psi\|_{L_2(\Gamma)}^2 = 1.
 \end{aligned}$$

The last inequality in (3.16) holds thanks to the condition $\int_{\Gamma} \psi \, ds = 0$.

3.5. Bounding the edge terms. We now bound the edge terms in (3.8), $p^{-1}h_T^{-2/p}\|\psi^e - I_h \psi\|_{L_p(e)}^2$. Assume that e is an edge of the element $T \in \mathcal{F}$. We begin by again applying Hölder’s inequality and (2.7) to compute

$$\begin{aligned}
 h_T^{-1/p}\|\psi^e - I_h \psi\|_{L_p(e)} &\lesssim h_T^{-1/p}\|\psi^e - (I_h \psi)^e\|_{L_p(e)} + \|(I_h \psi)^e - I_h \psi\|_{L_{\infty}(e)} \\
 (3.17) \qquad &\lesssim h_T^{-1/p}\|\psi^e - (I_h \psi)^e\|_{L_p(e)} + h_T^{\frac{1}{2}}\|\nabla(I_h \psi)\|_{L_2(\omega_{S_T})} \\
 &\lesssim h_T^{-1/p}\|\psi^e - (I_h \psi)^e\|_{L_p(e)} + \|\psi\|_{H^{3/2}(\omega_{S_T})}.
 \end{aligned}$$

Observe next that while $\Phi(\varphi^{-1}(\widetilde{T}))$ is flat (a subset of a plane), it is not necessarily true that $\Phi(\varphi^{-1}(p(e)))$ is a line segment. We must thus apply a somewhat different flattening argument than above. Let \mathbb{P} now be the plane containing the (flat) element T containing the edge e . Although the element T itself may have diameter $\ll h_T$, the

shape regularity of \mathcal{T} guarantees that there is a shape regular triangle V lying in \mathbb{P} but not necessarily in \mathcal{F} such that $\text{diam}(V)$ is equivalent to h_T and $T \subset V \subset \omega_{S_T}$. Equation (2.6) of Assumption 2 and the latter inclusion also imply that $p(V) \subset \omega'_{S_T}$.

The normal projection $p : V \rightarrow \Gamma$ has uniformly bounded gradient on V with $(\nabla p)^{-1}$ uniformly bounded on any tangent plane of $p(V)$, i.e., p is a smooth diffeomorphism on V . Let now $\varphi : \widehat{V} \rightarrow V$ be a standard affine reference transformation, where \widehat{V} is the reference triangle in \mathbb{R}^2 . Because V is shape regular with diameter h_T , we have $\|\nabla\varphi\| \lesssim h_T$ and $\|\nabla\varphi^{-1}\| \lesssim h_T^{-1}$. Writing $\rho = \psi - I_h\psi$ and $\widehat{\rho}^e = \rho^e \circ \varphi$ as before, we then have

$$(3.18) \quad h_T^{-1/p} \|\psi^e - (I_h\psi)^e\|_{L_p(e)} \lesssim \|\widehat{\rho}^e\|_{L_p(\varphi^{-1}(e))}.$$

We now use a trace inequality in order to bound the one-dimensional edge term by a two-dimensional norm. Let μ be a cutoff function which is 1 on \widehat{V} and 0 outside of a fixed ball containing \widehat{V} and which is uniformly bounded in C^2 . We first apply the extension operator described in Lemma 2.6 and then apply (2.12) with $n = 1$ and p as above. Following that, we apply the trace inequality (2.13) with $k = 1$, $n = 2$, and $s = 1/2$ (so that $s + (n - k)/2 = 1$) and then finally the bound (2.14) for the extension operator E . Letting \widehat{L} be the line containing $\varphi^{-1}(e)$, we thus obtain

$$(3.19) \quad \begin{aligned} \|\widehat{\rho}^e\|_{L_p(\varphi^{-1}(e))} &\lesssim \|\mu E \widehat{\rho}^e\|_{L_p(\widehat{L})} \\ &\lesssim \sqrt{p} \|\mu E \widehat{\rho}^e\|_{H^{1/2}(\widehat{L})} \\ &\lesssim \sqrt{p} \|\mu E \widehat{\rho}^e\|_{H^1(\mathbb{R}^2)} \\ &\lesssim \sqrt{p} \|E \widehat{\rho}^e\|_{H^1(\mathbb{R}^2)} \\ &\lesssim \sqrt{p} \|\widehat{\rho}^e\|_{H^1(\widehat{V})}. \end{aligned}$$

Combining (3.18) and (3.19) with a scaling argument yields

$$(3.20) \quad p^{-1/2} h_T^{-1/p} \|\psi^e - (I_h\psi)^e\|_{L_p(e)} \lesssim h_T^{-1} \|\rho^e\|_{L_2(V)} + \|\nabla_{\mathbb{P}} \rho^e\|_{L_2(V)}.$$

Recall next that from Assumption 2 it follows that $p(V) \subset \omega'_{S_T}$. Using the equivalence of norms on V and $p(V)$, we thus have

$$(3.21) \quad h_T^{-1} \|\rho^e\|_{L_2(V)} + \|\nabla_{\mathbb{P}} \rho^e\|_{L_2(V)} \lesssim \sum_{S \in \omega'_{S_T}} h_T^{-1} \|\rho\|_{L_2(\widetilde{T}_S)} + \|\nabla_{\Gamma} \rho\|_{L_2(\widetilde{T}_S)}.$$

We next compute as in (3.11) (with $p = 2$ and taking into account the fact that $\nabla \widehat{\rho}$ is equivalent to $h_T^{-1} \nabla_{\Gamma_h} \rho$), employ (2.13) with $k = 2$, $n = 3$, and $s = 1$ (so $s + (n - k)/2 = 3/2$), and then recall (2.14) to obtain for $S \in \omega'_{S_T}$

$$(3.22) \quad \begin{aligned} \|\nabla_{\Gamma} \rho\|_{L_2(\widetilde{T}_S)} &\lesssim \|E \widehat{\rho} \circ \Phi^{-1}\|_{H^1(\Phi(\varphi^{-1}(\widetilde{T}_S)))} \lesssim \|E \widehat{\rho} \circ \Phi^{-1}\|_{H^{3/2}(\mathbb{R}^3)} \\ &\lesssim \|\widehat{\rho}\|_{H^{3/2}(\widehat{K})} \lesssim \|\psi\|_{H^{3/2}(\omega_S)}. \end{aligned}$$

The last inequality in (3.22) was shown in (3.13). Employing (3.11), (3.12), and (3.13) also directly yields

$$(3.23) \quad h_T^{-1} \|\rho\|_{L_2(\widetilde{T}_S)} \lesssim \|\psi\|_{H^{3/2}(\omega_S)}.$$

Inserting (3.23) and (3.22) into (3.21) and finally into (3.20) yields

$$(3.24) \quad p^{-1/2} h_T^{-1/p} \|\psi^e - (I_h\psi)^e\|_{L_p(e)} \lesssim \|\psi\|_{H^{3/2}(\omega'_{S_T})},$$

which when combined with (3.17) yields

$$(3.25) \quad p^{-1/2} h_T^{-1/p} \|\psi^e - I_h \psi\|_{L_p(e)} \lesssim \|\psi\|_{H^{3/2}(\omega''_{S_T})}.$$

Employing the finite overlap of the patches ω''_{S_T} finally yields

$$(3.26) \quad \begin{aligned} \sum_{T \in \mathcal{F}} p^{-1} \sum_{e \subset \partial T} h_T^{-2/p} \|\psi^e - I_h \psi\|_{L_p(e)}^2 &\lesssim \|\psi\|_{H^{3/2}(\mathbb{R}^3)}^2 \lesssim \|\psi\|_{H^1(\Gamma)}^2 \\ &\lesssim \|\nabla_{\Gamma} \psi\|_{L_2(\Gamma)}^2 = 1. \end{aligned}$$

3.6. Completing the proof. Inserting (3.16) and (3.26) into (3.8), we obtain

$$(3.27) \quad \begin{aligned} \int_{\Gamma_h} (f_h + \Delta u_h)(\psi^e - I_h \tilde{\psi}) \, ds_h - \frac{1}{2} \sum_{T \in \mathcal{F}} \int_{\partial T} \llbracket \nabla_{\Gamma_h} u_h \rrbracket (\psi^e - I_h \tilde{\psi}) \, dr \\ \lesssim \left(\sum_{T \in \mathcal{F}} \eta_p(T)^2 \right)^{1/2}. \end{aligned}$$

We recall identity (2.2.19) from [8], $\nabla_{\Gamma} u_h^{\ell} = [\mathbf{I} - d\mathbf{H}]^{-1} [\mathbf{I} - \frac{\nu_h \otimes \nu}{\nu_h \cdot \nu}] \nabla_{\Gamma} u_h$, so that applying Hölder’s inequality and recalling that $\|\nabla_{\Gamma} \psi\|_{L_2(\Gamma)} = 1$ we obtain

$$(3.28) \quad \begin{aligned} \int_{\Gamma} [\mathbf{P} - \mathbf{A}_h^{\ell}] \nabla_{\Gamma} u_h^{\ell} \nabla_{\Gamma} \psi \, ds &\leq \|[\mathbf{P} - \mathbf{A}_h^{\ell}] \nabla_{\Gamma} u_h^{\ell}\|_{L_2(\Gamma)} \|\nabla_{\Gamma} \psi\|_{L_2(\Gamma)} \\ &= \|\mathbf{B}_h \nabla_{\Gamma_h} u_h\|_{L_2(\Gamma_h)}. \end{aligned}$$

Finally,

$$(3.29) \quad \begin{aligned} \int_{\Gamma_h} (f^e \mu_h - f_h) \psi \, ds_h &\leq \|\sqrt{\mu_h} f^e - f_h / \sqrt{\mu_h}\|_{L_2(\Gamma_h)} \|\sqrt{\mu_h} \psi^e\|_{L_2(\Gamma_h)} \\ &= \|\sqrt{\mu_h} f^e - f_h / \sqrt{\mu_h}\|_{L_2(\Gamma_h)} \|\psi\|_{L_2(\Gamma)} \\ &\leq C_2 \|\sqrt{\mu_h} f^e - f_h / \sqrt{\mu_h}\|_{L_2(\Gamma_h)} \|\nabla_{\Gamma} \psi\|_{L_2(\Gamma)} \\ &= C_2 \|\sqrt{\mu_h} f^e - f_h / \sqrt{\mu_h}\|_{L_2(\Gamma_h)}. \end{aligned}$$

Inserting (3.27), (3.28), and (3.29) into (3.7) completes the proof of Theorem 3.1.

4. Comments on efficiency.

4.1. Standard efficiency results. We begin by quoting efficiency results (a posteriori lower bounds) typical for residual-type error estimators for elliptic problems. Assuming momentarily that u and u_h solve an elliptic problem and the corresponding finite element equations, respectively, on a Euclidean domain, a standard result is

$$(4.1) \quad \begin{aligned} h_T \|f + \Delta u_h\|_{L_2(T)} + h_T^{1/2} \|\llbracket \nabla u_h \rrbracket\|_{L_2(\partial T)} \\ \lesssim \|\nabla(u - u_h)\|_{L_2(\omega_{edge,T})} + \sum_{T' \in \omega_T} h_T \|f - f_{T'}\|_{L_2(T')}. \end{aligned}$$

Here $\omega_{edge,T}$ is the patch of all elements sharing at least an edge with T and f_T is a suitable polynomial approximation to f on T , e.g., the average value of f over T in the case of piecewise linear finite element spaces. $h_T \|f - f_{T'}\|_{L_2(T')}$ is the data oscillation term and is of higher order so long as f is piecewise smooth on the mesh. When considering only the volumetric residual, a slightly more local (elementwise) result holds:

$$(4.2) \quad h_T \|f + \Delta u_h\|_{L_2(T)} \lesssim \|\nabla(u - u_h)\|_{L_2(T)} + h_T \|f - f_T\|_{L_2(T)}.$$

An analogue of (4.1) in which geometric terms also appear holds for surface finite elements on shape regular surface meshes; cf. [8]. However, the standard proofs of such estimates do not carry over to the irregular meshes considered here. On the other hand, in our numerical experiments below the indicators (3.1) and (3.2) do satisfy an efficiency property similar to (4.1). Below we give some theoretical explanation for this experimental observation, although full efficiency results are so far missing.

4.2. Efficiency of the volume residual. In this section we provide a nonstandard argument that the volume residual is generally bounded above by the error, up to higher order terms of geometric and data oscillation type.

With slight modification of the argument in [8, equation (3.3.27)], we first obtain the following proposition.

PROPOSITION 4.1. *Assume that $T \in \mathcal{F}$ is shape regular with diameter equivalent to h_T . Then*

$$(4.3) \quad \begin{aligned} h_T \|f_h + \Delta_{\Gamma_h} u_h\|_{L_2(T)} &\lesssim \|\nabla_{\Gamma}(u - u_h^{\ell})\|_{L_2(p(T))} + \|\mathbf{B}_h \nabla_{\Gamma_h} u_h\|_{L_2(T)} \\ &+ h_T \|f^e \mu_h - f_T\|_{L_2(T)} + h_T \|\mu_h f^e - f_h\|_{L_2(T)}. \end{aligned}$$

Here f_T is the average value of $f^e \mu_h$ on T . The last three terms $\|\mathbf{B}_h \nabla_{\Gamma_h} u_h\|_{L_2(T)}$, $h_T \|f - f_T\|_{L_2(T)}$, and $h_T \|\mu_h f^e - f_h\|_{L_2(T)}$ are all generally of higher order, so (4.3) is in effect very similar to the Euclidean result (4.1).

We now argue that even though we cannot expect (4.3) to hold for irregular elements T in \mathcal{F} having area $\ll h_T^2$, we can instead obtain a *patchwise* efficiency result, at least if f is sufficiently regular. Two facts work to our advantage in proving this result. First, $\Delta_{\Gamma_h} u_h = 0$ in the present case of piecewise linear FEMs and second, there is always a shape regular element of size h_T “close” to any element $T \in \mathcal{F}$. We now formalize the latter statement.

PROPOSITION 4.2. *Assume that $T \in \mathcal{F}$, and let $\tilde{\omega}_T = \omega_{S_T} \cap \Gamma_h$. Then there is an element $T_1 \subset \tilde{\omega}_T$ ($T_1 \in \mathcal{F}$) such that T_1 is shape regular and $\text{diam}(T_1) \gtrsim h_T$.*

Proof. The shape regularity of the outer mesh \mathcal{T} implies that the area of $\tilde{\omega}_T$ is uniformly equivalent to h_T^2 . To prove this, note that shape regularity of \mathcal{T} implies that there is a constant c such that for any point $x \in \tilde{T}$, the (three-dimensional) ball $B_{ch_T}(x) \subset \omega_{S_T}$. This guarantees that $\text{area}(\omega_T) \gtrsim h_T^2$. On the other hand, the number of elements in ω_{S_T} is bounded by shape regularity, and the intersection of Γ_h with each element in ω_{S_T} has area at most h_T . This proves the upper bound.

Shape regularity of \mathcal{T} also implies that the number of elements in \mathcal{F} intersecting ω_{S_T} is uniformly bounded above, so at least one of these elements T' must have area $\gtrsim h_T^2$. In addition, T' must also be shape regular, since it has diameter $\lesssim h_T$. \square

We finally state and prove our efficiency result, then make some remarks concerning its structure.

LEMMA 4.3. *Let $f_{h,T}$ be the average value of f_h over T . With assumptions as above,*

$$\begin{aligned}
 (4.4) \quad h_T \|f_h + \Delta_{\Gamma_h} u_h\|_{L_2(T)} &\lesssim \|\nabla_{\Gamma}(u - u_h^\ell)\|_{L_2(p(\tilde{\omega}_T))} \\
 &\quad + \sum_{T' \in \tilde{\omega}_T} [h_T \|\mu_h f^e - f_{T'}\|_{L_2(T')} + h_T \|\mu_h f^e - f_h\|_{L_2(T')}] \\
 &\quad + \|\mathbf{B}_h \nabla_{\Gamma_h} u_h\|_{L_2(T)} + \max_{T' \in \tilde{\omega}_T} h_T^2 |f_{h,T'} - f_{h,T}|.
 \end{aligned}$$

Proof. Let $T' \in \tilde{\omega}_T$ be the shape regular element of size h_T described in Proposition 4.2. Recall that h_T and $h_{T'}$ are equivalent by the shape regularity of \mathcal{T} . Then noting that $\Delta_{\Gamma_h} u_h = 0$, applying Hölder’s inequality while recalling that $|T|^{1/2} \lesssim h_T$, applying an inverse inequality on the shape-regular element T' , and finally making use of (4.3) yields

$$\begin{aligned}
 (4.5) \quad h_T \|f_h + \Delta_h u_h\|_{L_2(T)} &= h_T \|f_h\|_{L_2(T)} \\
 &\leq h_T \|f_h - f_{h,T}\|_{L_2(T)} + h_T^2 |f_{h,T}| \\
 &\leq h_T \|f_h - f_{h,T}\|_{L_2(T)} + h_T^2 |f_{h,T} - f_{h,T'}| + h_T^2 |f_{h,T'}| \\
 &\lesssim h_T \|f_h - f_{h,T}\|_{L_2(T)} + h_T^2 |f_{h,T} - f_{h,T'}| + h_T \|f_{h,T'}\|_{L_2(T')} \\
 &\lesssim h_T \|f_h - f_{h,T}\|_{L_2(T)} + h_T^2 |f_{h,T} - f_{h,T'}| \\
 &\quad + h_T \|f_{h,T'} - f_h\|_{L_2(T')} + h_T \|f_h + \Delta_{\Gamma_h} u_h\|_{L_2(T')} \\
 &\lesssim h_T \|f_h - f_{h,T}\|_{L_2(T)} + h_T^2 |f_{h,T} - f_{h,T'}| \\
 &\quad + h_T \|f_{h,T'} - f_h\|_{L_2(T')} + \|\nabla_{\Gamma}(u - u_h^\ell)\|_{L_2(p(T'))} \\
 &\quad + \|\mathbf{B}_h \nabla_{\Gamma_h} u_h\|_{L_2(T')} + h_T \|f^e \mu_h - f_{T'}\|_{L_2(T')} \\
 &\quad + h_T \|\mu_h f^e - f_h\|_{L_2(T')}.
 \end{aligned}$$

Collecting terms and extending integrals over $\tilde{\omega}_T$ as necessary completes the proof of (4.4). \square

We now make a few comments about Lemma 4.3. First, the patch $\tilde{\omega}_T$ is *not* the patch of elements consisting of all elements in \mathcal{F} sharing an edge with T . Rather, this patch is based on the volume mesh. Letting ω_T be the set of elements in \mathcal{F} sharing a vertex with T , it is clear that $\omega_T \subset \tilde{\omega}_T$, but equality does not generally hold. However, in our numerical experiments below we check efficiency ratios for element patches ω_T and consistently achieve a bounded ratio of elementwise error indicators to the L_2 norm of the error integrated over the corresponding patch ω_T . This may indicate that our efficiency bounds could be tightened, but it also may indicate either that $\tilde{\omega}_T$ and ω_T generally coincide in our examples or that the element T' used in the proof above always may be taken within ω_T for the meshes in our examples.

Second, we emphasize that Lemma 4.3 holds for the coarsest estimator η_2 defined above. Again, this is confirmed by our computational results, which indicate that η_2 is efficient and reliable, although with upper and lower bounds that are slightly farther apart than for the sharper estimators η_p , $p \gg 2$.

Finally, we note that the term $\max_{T' \in \tilde{\omega}_T} h_T^2 |f_{h,T'} - f_{h,T}|$ is not standard in efficiency bounds. However, it is easy to see that it is of higher order if f is suffi-

ciently regular. For example, if $f_h \in W_\infty^1(\tilde{\omega}_T)$, then $\max_{T' \in \tilde{\omega}_T} h_T^2 |f_{h,T'} - f_{h,T}| \lesssim h_T^3 \|\nabla f_h\|_{L_\infty(\tilde{\omega}_T)}$.

5. Numerical tests. For the test problem we consider the Laplace–Beltrami equation on the unit sphere,

$$-\Delta_\Gamma u = f \quad \text{on } \Gamma,$$

with $\Gamma = \{\mathbf{x} \in \mathbb{R}^3 \mid \|\mathbf{x}\|_2 = 1\}$ and the bulk domain $\Omega = (-2, 2)^3$.

The solution and the source term in spherical coordinates are given by

$$(5.1) \quad u = \sin^\lambda \theta \sin \phi, \quad f = (\lambda^2 + \lambda) \sin^\lambda \theta \sin \phi + (1 - \lambda^2) \sin^{\lambda-2} \theta \sin \phi.$$

One also verifies

$$\nabla_\Gamma u = \sin^{\lambda-1} \theta \left(\frac{1}{2} \sin 2\phi (\lambda \cos^2 \theta - 1), \sin^2 \phi (\lambda \cos^2 \theta - 1) + 1, -\frac{1}{2} \lambda \sin 2\theta \sin \phi \right)^T.$$

In [8] and [3] the choice is $\lambda = 0.6$. For $\lambda < 1$ the solution u is singular at the north and south poles of the sphere so that $u \in H^1(\Gamma)$, but $u \notin H^2(\Gamma)$.

Computational experiments were carried out using the software package DROPS [10], and all visualizations were done with the help of the open-source package Paraview [24]. In Table 5.1 we compute the H^1 norms of the surface finite element error for the *uniform* refinement of the outer triangulation. Here l is the refinement level as described in [22, p. 3355]. It holds that $h_T \leq \sqrt{3} 2^{-l}$. As expected, the optimal convergence order of $O(h)$ in H^1 is observed for $\lambda = 1$, while for the smaller values of λ the convergence order is suboptimal and decreases as $\lambda \rightarrow 0$. Similar results were observed for the convergence rates in L^2 norm (not shown), which also decreased from optimal $O(h^2)$ for $\lambda = 1$ to suboptimal $O(h^\alpha)$, $\alpha \in [1.36, 1.5]$ for $\lambda = 0.4$. Thus adaptive mesh refinement is desirable.

In our adaptive code we implemented the residual estimator $\eta_{p,\Gamma}^2 = \sum_{T \in \mathcal{F}} \eta_p(T)^2$. The additional geometric terms in (3.5) were ignored as their effects are known to be higher order. Doing so had no apparent effect on convergence for this example with simple geometry, though as demonstrated in [8], geometric error terms should be included on surfaces with regions having high curvature. We consider $p = 2$, $p = 10$, and $p = \infty$ in (3.2) and always assume $C_p = 1$. The assumption $C_p = 1$ is not warranted by our theory but rather was used to test whether our estimates might hold for the limiting case $p = \infty$. We employed a “maximum” marking strategy in which all volume tetrahedras S_T from \mathcal{T}_{Γ_h} with $\eta_p(T) > \frac{1}{2} \max_{T \in \mathcal{F}} \eta_p(T)$ are marked for further refinement. The refinement procedure in DROPS uses the algorithm from [19]. The initial volume mesh in our computations was obtained by the uniform triangulation of $(-1, 1)^3$; it consists of 48 tetrahedras with $h_S = \sqrt{3}$ resulting in 15 surface d.o.f., i.e., $\dim(V_h^\Gamma) = 15$.

TABLE 5.1

Uniform refinement: the H^1 seminorms of the error, $\|\nabla_{\Gamma_h}(u^e - u_h)\|_{L^2(\Gamma_h)}$, and convergence order for various values of the exponent λ .

l	#d.o.f.	$\lambda = 0.4$		$\lambda = 0.6$		$\lambda = 0.8$		$\lambda = 1.0$	
2	100	1.21e-0	–	6.85e-1	–	4.13e-1	–	3.31e-1	–
3	448	9.38e-1	0.367	4.46e-1	0.619	2.16e-1	0.935	1.55e-1	1.094
4	1864	7.24e-1	0.374	2.98e-1	0.582	1.21e-1	0.836	7.76e-2	0.998
5	7552	5.56e-1	0.381	1.99e-1	0.583	6.80e-2	0.831	3.85e-2	1.011
6	30412	4.26e-1	0.384	1.33e-1	0.581	3.87e-2	0.813	1.95e-2	0.981
7	121708	3.25e-1	0.390	8.86e-2	0.586	2.20e-2	0.815	9.72e-3	1.004

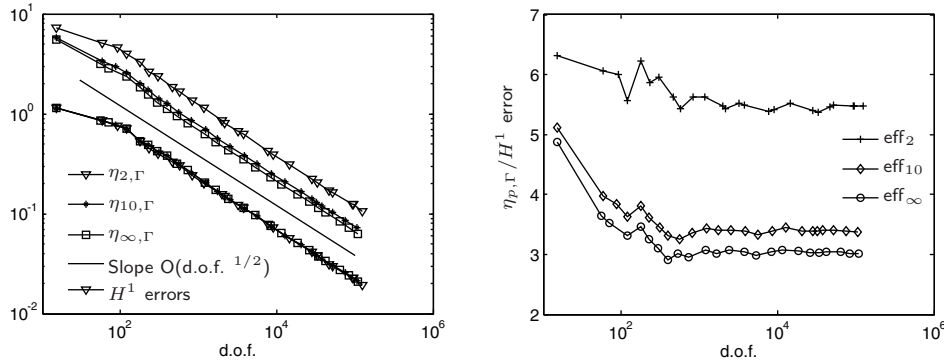


FIG. 5.1. Decrease of the error and error indicators (left) and global efficiency $\eta_{p,\Gamma}/\|\nabla_{\Gamma}(u - u_h^\epsilon)\|_{L_2(\Gamma)}$ (right) for the adaptive algorithm with $p = 2$, $p = 10$, and $p = \infty$.

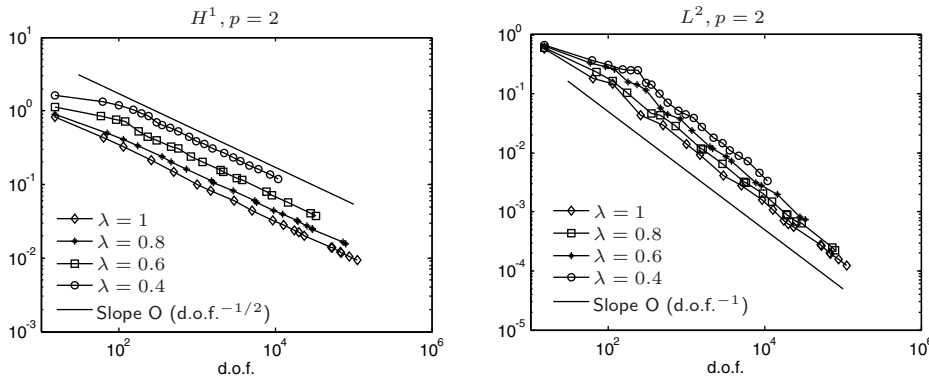


FIG. 5.2. Decrease of the error in H^1 norm (left) and L^2 norm (right) for the adaptive algorithm ($p = 2$) within 20 refinement steps for various values of λ .

5.1. Reliability and global efficiency. Results produced by the adaptive algorithm with $\lambda = 0.6$ and $p = 2$, $p = 10$, and $p = \infty$ are displayed in Figure 5.1. In the left plot the error decrease is displayed, and in the right plot the ratio of the error estimators $\eta_{p,\Gamma}$ to the resulting global error is displayed. Here we see that all three estimators lead to optimal order error decrease, and in fact the error lines for the AFEM based on the three estimators are essentially indistinguishable. Using larger p does, however, lead to slightly more accurate estimation of the error, at least if C_p is taken to be 1.

Figure 5.2 shows the decrease of the error within 20 steps of the refinement algorithm for various values of the exponent λ . We notice that for more singular solutions, more refinement steps are needed to get the error under a desired tolerance; however, for all tested values the convergence rate stays optimal with respect to the number of d.o.f. Although we have not studied in this paper estimates and indicators for the L^2 norm of the error, we show in the right plot the convergence history for it and observe that the rate appears optimal for the L^2 norm as well.

Figure 5.3 displays a cutaway view which includes both the adaptively refined bulk and surface meshes. The meshes are shown for the ninth refinement level and consists of 11,632 volume tetrahedra; 3525 of them are intersected by Γ_h , resulting in $\dim(V_h^\Gamma) = 1172$. Figure 5.4 displays the surface mesh near the north pole magnified

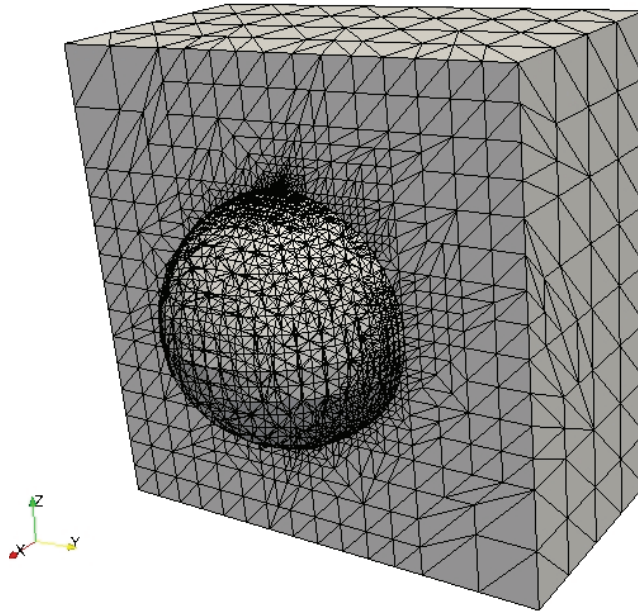


FIG. 5.3. *Cutaway visualization of the volume and surface meshes with refinement at the north pole.*

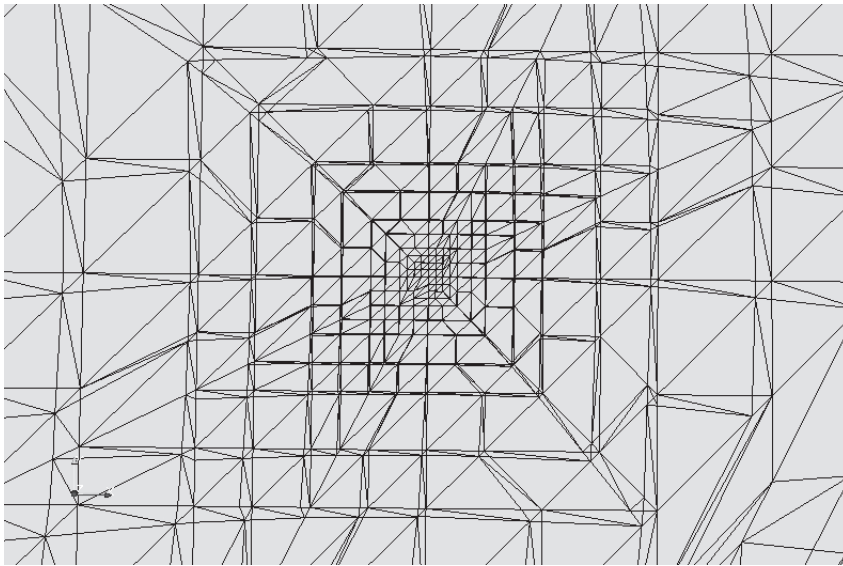
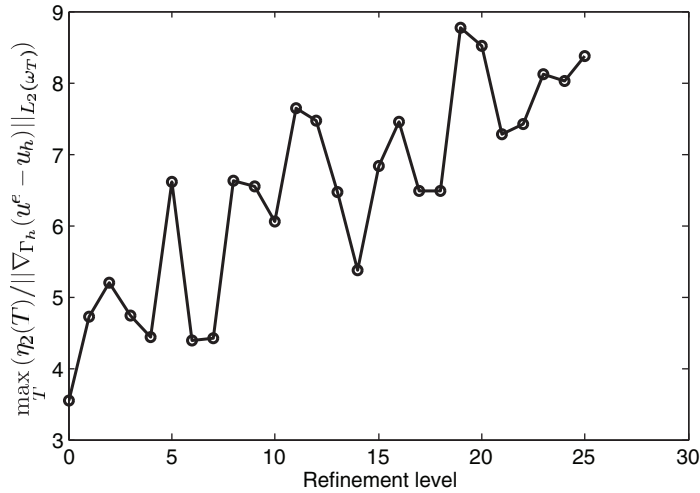


FIG. 5.4. *Visualization of the refinement near the north pole, zoomed in 20 \times .*

20 times. This mesh clearly displays the irregularity typical of our algorithm; note the presence both of highly anisotropic (long, thin) elements and of very small elements sharing vertices with much large elements. Neither of these characteristics is present in shape regular meshes, and they correspondingly make our analysis more challenging.

FIG. 5.5. Local efficiency for $p = 2$.

5.2. Local efficiency. Our goal in this subsection is to test whether, and for what values of p , the local efficiency result $\eta_p(T) \lesssim \|\nabla_{\Gamma}(u - u_h^{\ell})\|_{L_2(\omega_T)} + \text{h.o.t.}$ holds, where h.o.t. are higher order terms consisting of geometric and data oscillation terms as in (4.4). We also illustrate the efficiency estimate (4.4) for the volume residual.

We first describe two local efficiency tests for $p = 2$. First we checked the ratio $h_T \|f + \Delta_{\Gamma_h} u_h\|_{L_2(T)} / \|\nabla_{\Gamma_h}(u^e - u_h)\|_{L_2(T)}$ for a heavily refined mesh (refinement level $n = 23$). The maximum ratio over the mesh was about 400. Thus we conclude that (4.3) does not hold for general elements. We then tested the ratio $\eta_2(T) / \|\nabla_{\Gamma_h}(u^e - u_h)\|_{L_2(\omega_T)}$. As can be observed in Figure 5.5, there is some increase in the maximum ratio as the mesh is refined, but the increase appears to level off at a value of around 9. This experiment confirms the correctness of Lemma 4.3 and also strongly indicates that even with the coarser scaling used in η_2 , the edge (jump) residual terms yield an efficient as well as a reliable approximation to the true error, although sometimes with constants that are not very close to 1.

Note that η_p is nonincreasing in p , which implies that if a given efficiency estimate $\eta_p(T) \lesssim \|\nabla_{\Gamma_h}(u^e - u_h)\|_{L_2(\omega_T)} + \text{h.o.t.}$ does *not* hold for $p = \infty$, then it will also not hold for finite values of p in $[2, \infty)$. Thus although $p = \infty$ is not included in our reliability theory, as above it still provides an interesting computational test case for purposes of comparison. We repeated both tests here that were carried out for the case $p = 2$. First checking the ratio $|T|^{1/2} \|f + \Delta_{\Gamma_h} u_h\|_{L_2(T)} / \|\nabla_{\Gamma_h}(u^e - u_h)\|_{L_2(T)}$ for a heavily refined mesh (mesh level $n = 23$) as above, we found a maximum ratio of about 9. This indicates that the volume portion of the error indicator η_{∞} is in fact elementwise efficient in the sense of (4.3), though we do not have proof. In addition, the maximum ratio over the mesh of element indicators to patchwise errors $\eta_{\infty}(T) / \|\nabla_{\Gamma_h}(u^e - u_h)\|_{L_2(\omega_T)}$ was about 4.

These local efficiency experiments, along with the global efficiency experiments in the preceding section, indicate that using the sharper scaling in the indicators η_p , $p > 2$, has only moderate advantages. The constants in the patchwise efficiency and global reliability estimates appear to be a factor of about two times better when using the most extreme scaling $p = \infty$ (which again is not allowed by our theory). While this gain is of some importance with respect to the ability of estimators to give reasonable error estimates, there appears to be essentially no gain at all in the ability

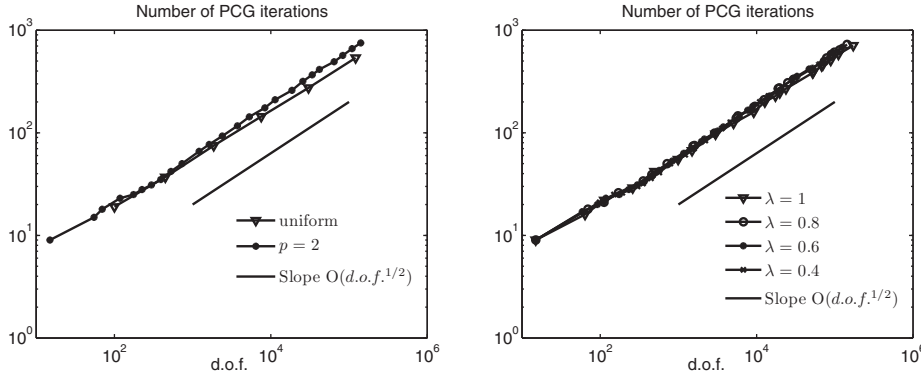


FIG. 5.6. Growth in the number of CG iterations: Comparison between uniform and adaptive refinement ($p = 2$) (left) and for adaptive refinement for varying singularity strengths (right).

of the resulting AFEM to reduce the error when using sharper error indicators. This reinforces an important fact about the surface FEM defined in [22] and studied here: it is the approximation properties of the outer bulk mesh that are inherited by the surface FEM.

5.3. Efficiency of linear solvers. We finally briefly comment on the efficiency of the linear solvers used in our computations. Consider the system of functions from V_h^Γ which are traces of outer nodal basis functions; only nodal functions with non-zero traces contribute to the system. Clearly this system spans V_h^Γ and, following [22], we use it to decompose the surface solution u_h and to build finite element stiffness matrices. The resulting stiffness matrix can be rank deficient, with an at most two-dimensional kernel. However, since the finite element problem (2.3) is well-posed (subject to zero mean conditions), the corresponding algebraic system is always consistent. The discrete surface Γ_h cuts the outer tetrahedra in an arbitrary way; hence the support measure of the surface basis functions can vary from (almost) zero to the full size $O(h_T^2)$. Thus diagonal scaling of resulting stiffness and mass matrices is necessary even for a regular bulk mesh. A detailed study of matrix properties of the surface finite element method that we use here is given in [23] for the case of regular mesh refinement, i.e., quasi-uniform meshes. There an *effective* spectral condition number of $O(|\ln h| h^{-2})$ is proved for the diagonally scaled stiffness matrix in the case of a one-dimensional surface embedded in \mathbb{R}^2 . (Here h is the mesh diameter of a quasi-uniform mesh.) Computational experiments confirm that this behavior carries over to the case of two-dimensional surfaces studied here.

For the current case of adaptively refined meshes we do not study the condition number directly, but instead use the number of conjugate gradient iterations as a proxy since this is the most important quantity in practice in any case. Our code employs a preconditioned conjugate gradient algorithm with a symmetric Gauss-Seidel preconditioner applied to diagonally scaled matrices. The iteration is stopped when the relative decrease of the residual reaches 10^{-9} . Note that the CG method applies to consistent linear algebraic systems even with rank deficient symmetric nonnegative definite matrices if the initial guess is from the appropriate subspace. (In our experiments we use the zero initial guess.) In this case, the number of CG iterations necessary to reach a given tolerance should scale as $\sqrt{\kappa}$, where κ is the effective condition number [4]. For uniform meshes, $h^{-2} \sim \text{d.o.f.}$, where d.o.f. is the number of

degrees of freedom in the surface mesh. Thus we expect that the number of CG iterations should be proportional to $\sqrt{\text{d.o.f.}}$ if the behavior is consistent with the uniform case. Experiments in Figure 5.6 show behavior consistent with this expectation. In the first plot, it is seen that the number of iterations required for the adaptive case grows slightly faster with respect to d.o.f. than in the case of uniform refinement, but it still is consistent with an $O(\sqrt{\text{d.o.f.}})$ scaling. In the second plot, we see that the behavior of the linear solvers for adaptively refined meshes is robust when the singularity strength is increased. Thus the behavior of the linear solvers is still standard for the surface FEM studied here even under adaptive refinement.

6. Conclusions and outlook. The surface FEM studied in this paper enjoys a posteriori error estimates largely resembling the ones for a standard FEM in a Euclidean domain. Although our analysis of the method is nonstandard, the resulting error indicator is simple, proved to be reliable, and shown numerically to be efficient. A straightforward adaptive strategy based on the indicator leads to optimal convergence rate in H^1 norm. Additional research is required to prove the numerically observed reliability of the $p = \infty$ indicator as well as the efficiency of the “jump” part of the indicator for $p \geq 2$.

Acknowledgments. We would like to thank Joerg Grande for his help in coding with the DROPS package and Russell Brown for helpful discussions concerning Lemma 2.3.

REFERENCES

- [1] D. ADALSTEINSSON AND J.A. SETHIAN, *Transport and diffusion of material quantities on propagating interfaces via level set methods*, J. Comput. Phys., 185 (2003), pp. 271–288.
- [2] R.A. ADAMS, *Sobolev Spaces*, Pure Appl. Math. 65, Academic Press, New York, 1975.
- [3] T. APEL AND C. PESTER, *Clement-type interpolation on spherical domains—interpolation error estimates and application to a posteriori error estimation*, IMA J. Numer. Anal., 25 (2005), pp. 310–336.
- [4] O. AXELSSON AND G. LINDSKOG, *The rate of convergence of the conjugate gradient method*, Numer. Math., 48 (1986), pp. 499–523.
- [5] M. BERTALMIO, L.T. CHENG, S. OSHER, AND G. SAPIRO, *Variational problems and partial differential equations on implicit surfaces: The framework and examples in image processing and pattern formation*, J. Comput. Phys., 174 (2001), pp. 759–780.
- [6] M. BURGER, *Finite element approximation of elliptic partial differential equations on implicit surfaces*, Comput. Vis. Sci., 12 (2009), pp. 87–100.
- [7] K. DECKELNICK, G. DZIUK, C.M. ELLIOTT, AND C.J. HEINE, *An h-narrow band finite-element method for elliptic equations on implicit surfaces*, IMA J. Numer. Anal., 30 (2010), pp. 351–376.
- [8] A. DEMLOW AND G. DZIUK, *An adaptive finite element method for the Laplace-Beltrami operator on implicitly defined surfaces*, SIAM J. Numer. Anal., 45 (2007), pp. 421–442.
- [9] A. DEMLOW, *Higher-order finite element methods and pointwise error estimates for elliptic problems on surfaces*, SIAM J. Numer. Anal., 47 (2009), pp. 805–827.
- [10] DROPS, <http://www.igpm.rwth-aachen.de/DROPS/>.
- [11] T. DUPONT AND R. SCOTT, *Polynomial approximation of functions in Sobolev spaces*, Math. Comp., 34 (1980), pp. 441–463.
- [12] G. DZIUK, *Finite elements for the Beltrami operator on arbitrary surfaces*, in Partial Differential Equations and Calculus of Variations, S. Hildebrandt and R. Leis, eds., Lecture Notes in Math. 1357, Springer, Berlin, 1988, pp. 142–155.
- [13] G. DZIUK AND C.M. ELLIOTT, *Surface finite elements for parabolic equations*, J. Comput. Math., 25 (2007), pp. 385–407.
- [14] G. DZIUK AND C.M. ELLIOTT, *Eulerian finite element method for parabolic equations on implicit surfaces*, Interfaces Free Bound., 10 (2008), pp. 119–138.
- [15] G. DZIUK AND C.M. ELLIOTT, *Finite elements on evolving surfaces*, IMA J. Numer. Anal., 27 (2007), pp. 262–292.

- [16] D. GILBARG AND N.S. TRUDINGER, *Elliptic Partial Differential Equations of Second Order*, 2nd ed., Springer-Verlag, Berlin, 1998.
- [17] J.B. GREER, *An improvement of a recent Eulerian method for solving PDEs on general geometries*, *J. Sci. Comput.*, 29 (2006), pp. 321–352.
- [18] P. GRISVARD, *Elliptic Problems in Nonsmooth Domains*, Monogr. Stud. Math. 24, Pitman, Boston, 1985.
- [19] S. GROSS AND A. REUSKEN, *Parallel multilevel tetrahedral grid refinement*, *SIAM J. Sci. Comput.*, 26 (2005), pp. 1261–1288.
- [20] D. JERISON AND C.E. KENIG, *The inhomogeneous Dirichlet problem in Lipschitz domains*, *J. Funct. Anal.*, 130 (1995), pp. 161–219.
- [21] V. MAZ'YA AND T. SHAPOSHNIKOVA, *On the Bourgain, Brezis, and Mironescu theorem concerning limiting embeddings of fractional Sobolev spaces*, *J. Funct. Anal.*, 195 (2002), pp. 230–238.
- [22] M.A. OLSHANSKII, A. REUSKEN, AND J. GRANDE, *A finite element method for elliptic equations on surfaces*, *SIAM J. Numer. Anal.*, 47 (2009), pp. 3339–3358.
- [23] M.A. OLSHANSKII AND A. REUSKEN, *A finite element method for surface PDEs: Matrix properties*, *Numer. Math.*, 114 (2010), pp. 491–520.
- [24] *Paraview*, <http://www.paraview.org/>.
- [25] R. VERFÜRTH, *A posteriori error estimators for convection-diffusion equations*, *Numer. Math.*, 80 (1998), pp. 641–663.